ANALYSIS OF CRACKED PRESSURE VESSEL NOZZLES BY FINITE ELEMENTS

J. REYNEN

Division Technologie, J.R.C. Euratom, I-21020 Ispra (Varese), Italy; Commission of the European Communities

SUMMARY

In order to assess the safety of pressure vessel nozzles, the analyses should take into account cracks. The Fracture Mechanics (FM) concept provides adequate tools to deal with the prediction of brittle type of failure, as well as the correlation of crack growth due to fatigue and/or stress corrosion. To this end the crack and its local stress field are characterized by the stress intensity fractors K_I, K_{II} and K_{III} for the three loading modes. The stress intensity factors are defined by the (hypothetical) stress singularity at the crack tip according to classical elasticity theory. For standard cracks and loadings the engineer has at his disposal handbooks.

For more realistic crack geometries recourse is to be made to numerical stress analysis techniques like the finite element method. Rather then trying by means of an extremely fine mesh at the crack tip to approach the singular stress and/or displacement field it has been shown to be more efficient to use energy method to define the strain energy release rates G_I, G_{II} and G_{III} from the variation of potential energy with increasing crack area.

The paper describes various algorithms, their computer implementations and relative merits to define in an effective way strain energy release rates along the tip front of arbitrary 3 D cracks under arbitrary load including thermal strains. These techniques are basically equivalent to substructuring techniques and consequently they can be implemented to any FEM program able to deal with the data handling problems of the substructuring technique. Special finite elements with a built-in stress-singularity are not necessary although their use contributes to accuracy and the mesh can be coarser. Examples are given carried out with a substructure version of the BERSAFE system. These examples include a corner crack in a pressure vessel nozzle loaded by internal pressure and by thermal stresses. Although not of any fundamental importance, in practice the difficulties consist in generating an appropriate mesh to represent the crack front.

For the example of the corner crack in a nozzle the problem has been solved by developing a special purpose mesh generation program (EURCRACK).

1. INTRODUCTION

Although in the engineering community, the stress intensity factors K_I, K_{II}, K_{III} are now commonly used to characterise cracks with corresponding loads, they remain rather artificial parameters, due to their obscure dimensions ($N\,m^{-3/2}$). An alternative and more fundamental parameter has already been indicated by Griffith[1, 2], who postulated that on the onset of brittle crack propagation the surface energy γ is related to the variation of free energy (in mechanics known as the potential energy Π) by a balance for a virtual crack area increase δA:

$$\gamma \delta A + \frac{\partial \Pi}{\partial A} \delta A = 0 \qquad (1)$$

This equation suggests the introduction of the strain energy release rate G to be compared to a critical value G_C:

$$G = -\frac{\partial \Pi}{\partial A}, \quad G < G_C \qquad (2)$$

It has been shown[3] that this energy postulate is basically equivalent to the inverse square root stress singularity model of Irwin[4]. Various analytical expressions have been formulated for G, of which the most known are the contour integrals around the crack tip singularity[3, 5], known as J integral. In a similar way as for stress intensity factors, one introduces three strain energy release rates for the three modes. The relations between K_N and G_N are[4]:

$$G = G_I + G_{II} + G_{III} = -\frac{\partial \Pi}{\partial A}$$
$$E' G_I = K_I^2, \quad E' G_{II} = K_{II}^2, \quad E G_{III} = K_{III}^2 (1 + \nu) \qquad (3)$$
$$E' = E \quad \text{(plane stress)}, \quad E \text{ Young's modulus}$$
$$E' = E/(1 - \nu^2) \quad \text{(plane strain)}, \quad \nu \text{ Poisson's ratio}$$

Additional symmetry conditions on the virtual crack area increase δA enables to separate the three modes in eq. (3).

For actual FM applications the engineer has at his disposal handbooks[6, 7], giving for standard crack geometries and loadings the stress intensity factors in tabulated and/or graphical form. They have been defined from analytical and/or numerical solutions of classical elasticity theory formulations of the singular stress field around the crack tip. For more realistic crack geometries and loadings, the handbooks are of limited use, and recourse is to be made to numerical stress analysis techniques like the finite element method (FEM)[8]. Rather than trying by means of an extreme fine mesh to produce the singular stress field and/or the displacement field around the crack tip and from these the corresponding stress intensity factors, it has been shown to be more efficient to define the strain energy release rates from potential energy variation with crack area[9-16].

The present paper deals with the problem of strain energy release rates of cracks

in nozzles. The calculations have been carried out by a substructure version[15] of the BERSAFE system[17]. Temperature distributions have been calculated by the program FLHE[18]. The finite element meshes of the cracked nozzle have been generated automatically by the program EURCRACK[19].

2. STRAIN ENERGY RELEASE RATES

In a recent paper[16] the author has discussed various algorithms, and their computer implementations to calculate strain energy release rates [9-15], concluding that the stiffness derivative algorithm is the most attractive one for 3D cracks.

Consider for this the potential energy of a structure defined by the sum of internal strain energy and the potential energy of external forces. In terms of the FEM concept[8] it can be written as:

$$\Pi = \frac{1}{2}\int \{\varepsilon^e\}^T [D] \{\varepsilon^e\}\, dV - \{u\}^T \{f^1\} \qquad (4)$$

$\{u\}$ discretised displacement vector, $\{f^1\}$ discretised external load vector;

$\{\varepsilon^e\}$ elastic-strain vector, $[D]$ elasticity matrix relating stress to strain:

$$\{\sigma\} = [D]\{\varepsilon^e\} = [D](\{\varepsilon\} - \{\varepsilon^o\}) \qquad (5)$$

$\{\varepsilon\}$ total-strain vector, $\{\varepsilon^o\}$ initial-strain vector e.g. thermal strain $\{\alpha T\}$.

Introducing through a matrix $[B]$ the kinematic relations between strain and displacements, one obtains :

$$\{\varepsilon\} = [B]\{u\} \qquad (6), \quad \Pi = \frac{1}{2}\{u\}^T [K]\{u\} - \{u\}^T \{f\} + SET \qquad (7)$$

$$[K] = \int [B]^T [D] [B]\, dV \quad \text{(stiffness matrix)} \qquad (8)$$

$$\{f\} = \{f^o\} + \{f^1\} \quad \text{(total load vector)} \qquad (9)$$

$$\{f^o\} = \int [B]^T [D]\{\varepsilon^o\}\, dV \quad \text{(initial-strain loading vector)} \qquad (10)$$

$$SET = \frac{1}{2}\int \{\varepsilon^o\}^T [D]\{\varepsilon^o\} dV \quad \text{(initial-strain energy)} \qquad (11)$$

The term SET depends only on initial strains $\{\varepsilon^o\}$ and for constant initial strains, such as thermal strains, the term can be dropped since only variations of Π are to be considered. The variation of potential energy with crack area A becomes:

$$\frac{\partial \Pi}{\partial A} = \left\{\frac{\partial \Pi}{\partial u}\right\}^T \left\{\frac{\partial u}{\partial A}\right\} + \left[\frac{\partial \Pi}{\partial K}\right]^T \left[\frac{\partial K}{\partial A}\right] + \left\{\frac{\partial \Pi}{\partial f}\right\}^T \left\{\frac{\partial f}{\partial A}\right\} \qquad (12)$$

The variation of potential energy with $\{u\}$ is zero (equilibrium) and the last two terms remain:

$$G = -\frac{1}{2}\{u\}^T \left[\frac{\partial K}{\partial A}\right]\{u\} + \{u\}^T \left\{\frac{\partial f}{\partial A}\right\} \qquad (13)$$

The matrix $\left[\frac{\partial K}{\partial A}\right]$ is nearly empty since only degrees of freedom (DOF) belonging to the crack tip elements give contributions. Also the term $\left\{\frac{\partial f}{\partial A}\right\}$ corresponds only to variations

of load on crack tip elements. These terms are defined from the differences $[\delta K]$ and $\{\delta f\}$ for two adjacent crack tip positions. These differences are formed using the "adding" mechanism of the substructuring technique, by introducing for one of the crack tip positions negative Young's modulus and opposite loadings (if there are any). The effect of thermal strains is taken into account by $\{f^o\}$ according to eq. (10) and the opposite Young's modulus takes care of subtracting the two contributions. The matrix $[\delta K]$ and the load vector $\{\delta f\}$ are stored on the substructure tape. An auxiliary program GCAL3 reads this tape ($[\delta K]$ and $\{\delta f\}$) as well as the displacement tape $\{u\}$ to be prepared in a previous run with back substitution and carries out the multiplications of eq. (13). The change in area is defined according to Appendix 1. Special crack tip elements contribute to accuracy (Appendix 2).

3. CORNER CRACK IN PRESSURE VESSEL NOZZLE

3.1 Mesh Generation

A major practical problem in FEM is the generation of an appropriate mesh and in particular for 3D cases it is a tedious task and a source of errors when carried out by hand. Automatic mesh generation by means of a computer program solves the problem to a great extent. For the analysis of cracked pressure vessel nozzles a special purpose mesh-generation program EURCRACK[19] has been developed from the program EURCYL[20]. In EURCRACK a 2D mesh (Fig. 1) of the longitudinal plane of the vessel is transformed automatically into a 3D mesh of the nozzle (Fig. 2), taking care of fillet radii, reinforcement etc. Then this mesh is locally refined in order to represent the corner crack. To this end the four elements in the corner (see Fig. 1 and 2) are replaced by the 3D mesh of Fig. 3 which, on its turn, is generated automatically from the 2D mesh of Fig. 4. The 3D mesh of crack tip elements is represented in Fig. 5 and consists of 8 x 4 isoparametric elements with 15 nodes of the wedge type (Fig. 6). An option exists to generate elements with displaced side nodes in order to simulate the stress singularity at the crack tip (Appendix 2). The crack front is generated as a 1/4 ellips with half axes defined by input. The 1/4 ellips is described by the 8 sides (17 nodes) of the parabolic crack tip elements. For different crack fronts only the latter part has to be repeated.

3.2 Substructuring

The calculation of strain energy release rates can be made more efficient by employing substructuring techniques[15,16]. As is seen from eq. (13) only the displacements of nodes of elements lying on the crack front are needed for the calculation of G and consequently the back-substitution can be limited to these nodes. This is achieved by generating firstly a substructure of the nozzle (Fig. 2) without the elements near the crack. In the next run the substructure is assembled to the mesh of Fig. 3 and a back-substitution is carried out (only

for the nodes of Fig. 3). The formation of the 17 matrices $[\delta K]$ and the 17 vectors $\{\delta f\}$ is carried out in a subsequent run. For another crack front only the latter runs have to be repeated. In Table I the sequence of the calculations is represented, including typical computer times for the IBM 370/165, for both elastic and thermo-elastic analyses.

3.3 Results

Calculations have been carried out for a corner crack in a BWR nozzle for internal pressure and for a thermal load. The thermal boundary conditions are given in Fig. 7, including temperature distributions calculated by FLHE[18]. The resulting thermal stresses in the longitudinal plane of the uncracked nozzle are given in Fig. 8. In Fig. 9 are given the stresses due to an internal pressure of 90 bar. Strain energy release rates for the thermal and mechanical load are given in Fig. 10 (a=7, 8, 9, 10 cm). In order to check the accuracy of the stiffness derivative method, various virtual displacements have been employed. In general it is concluded that (for this case) a virtual crack area variation corresponding to $\delta a = .2\%$ of the side of the crack tip element gives the best results.

4. CONCLUSIONS

It has been shown that by means of substructuring techniques the calculation of strain energy release rates for 3D thermo-elastic crack problems is economically feasible. A major source for errors is the mesh generation which preferably should be carried out automatically.

5. ACKNOWLEDGEMENT

The author expresses his gratitude toward Messrs. Blanckenburg and De Windt, who have been in charge of the computer runs.

REFERENCES

[1] GRIFFITH, A.A., "The Phenomena of Rupture and Flow in Solids", Phil. Trans. Roy. Soc. London, Series A 221, 1920, p 163-1938

[2] GRIFFITH, A.A., "The Theory of Rupture", Proc. of 1st Int. Congress for App. Mech., Delft 1924, p 55-63

[3] SANDERS, J.L., "On the Griffith-Irwin Fracture Theory", J. of Appl. Mech., 27, 352 (1960)

[4] IRWIN, G.R., "Analysis of Stresses and Strains near the End of a Crack Transversing a Plate", ASME, J. Appl. Mech., 24, 361 (1957)

[5] RICE, J.R., "A Path-Independent Integral and the Approximate Analysis of Strain Concentrations by Notches and Cracks", J. Appl. Mech., 34, 287-298 (1967)

[6] PARIS, P., SIH, G., "Stress Analysis of Cracks", ASTM, 381, 30 (1965)

[7] TADA, H., PARIS, P.C., IRWIN, G., "The Stress Analysis of Cracks Handbook", Del Research Corp., 1973

[8] ZIENKIEWICZ, O.C., "The Finite Element Method in Engineering Science", McGraw Hill (1971)

[9] GILLMAN, J.D., RASHID, J.R., "Three-Dimensional Analysis of Reactor Pressure Vessel Nozzles", 1st SMIRT Conf., G 2/6, Berlin, 1971

[10] AAMODT, B., BERGAN, P.G., KLEM, H.F., "Calculation of Stress Intensity Factors and Fatigue Crack Propagation of Semi-Elliptical Part-Through Surface Cracks", 2nd Int. Conf. Pressure Vessel Techn., San Antonio, Texas, 1973, p 911-921

[11] BERGAN, P.G., AAMODT, B., "Finite Element Analysis of Crack Propagation in 3D Solids under Cyclic Loading", 2nd SMIRT Conf., Berlin, 1973, vol. G

[12] PARKS, D., "A Stiffness Derivative Finite Element Technique for Determination of Elastic Crack Tip Stress Intensity Factors", Int. J. of Fracture, 10 (Dec. 1974), p 487-502

[13] HELLEN, T., "The Calculation of Stress Intensity Factors Using Refined Finite Element Techniques", 2nd SMIRT Conf., Berlin, 1973

[14] HELLEN, T., "On the Method of Virtual Crack Extensions", Int. J. Num. M. in Eng., Vol. 9, 187-207 (1975)

[15] REYNEN, J., "A Substructure Version of "BERSAFE"; Finite Element Workshop Meeting, Sept. 1973, University of Stuttgart

[16] REYNEN, J., "On the Use of Finite Elements in the Fracture Analysis of Pressure Vessel Components", 2nd Nat. Congress on Pressure Vessels and Piping (ASME), San Francisco, June 1975

[17] HELLEN, T., "The Application of the BERSAFE Finite Element System to Nuclear Design Problems", 1st SMIRT Conf. (M), Berlin, 1971

[18] FULLARD, K., "FLHE: A Finite Element Program for the Calculation of Temperatures in Arbitrary Structures", 1st SMIRT Conf. (M), Berlin 1971

[19] DE WINDT, P., REYNEN, J., "EURCRACK - A Program to Generate Finite Element Meshes for Cracked Pressure Vessel Nozzles", EUR-Report 1975 (to be published)

[20] DE WINDT, P., REYNEN, J., "EURCYL - A Computer Program to Generate Finite Element Meshes for Pressure Vessel Nozzles", Level 2, EUR-5257-e

[21] MARCAL, P.V., STUART, P.M., BETTES, R.S., "Elastic Plastic Behaviour of a Longitudinal Semi-Elliptical Crack in a Thick Pressure Vessel", HSSTP - Tech. Rep. 28, Div. Eng. Brown Un., June 1973

[22] TRACEY, D., "Finite Elements for Three-Dimensional Elastic Crack Analysis", N.E. & D., 26 (1974) 282

[23] BENZLEY, S., "Representation of Singularities with Isoparametric Elements", Int. J. Num. M. Eng., 8 (1974) 537

[24] PIN TONG, PIAN, T., RASNEY, S., "A Hybrid-Element Approach to Crack Problems in Plane Elasticity", Int. J. Num. M. Eng., 7 (1973) 297

[25] BOND, T.J., Ph.D.-Thesis, University of Nottingham

[26] NEALE, B.K., "Finite Element Crack Analysis Using the J. Integral Method", CEGB Rep. RD/B/N2785 (1973), Int. J. of Fracture, 11 (1975)

[27] BLACKBURN, W.S., "Calculation of Stress Intensity Factors at Crack Tips Using Special Finite Elements", Math. of FEM, Brunel Un., 1972

[28] BARSOUM, R.S., Int. J. of Fracture,10 (1974), Int. J. of Fracture,11 (1975)

APPENDIX 1

For 2D problems the crack area A is uniquely defined by the crack length (a) and the strain energy release rate is constant along the crack front. For 3D problems the strain energy release rate varies along the crack front, and the characteristic length of the crack (a) has to be interpreted in the sense of a hydraulic diameter:

$$2a = 4A/\oint ds \tag{14}$$

Using this concept, the definition of strain energy release rate (eq. (2)) can now be written as:

$$\oint G(s)\delta a(s)ds = -\frac{\partial \Pi}{\partial A}\delta A \tag{15}$$

Here $\delta a(s)$ is the local increase in crack size along the crack front and δA the corresponding change in crack area. In order to define G(s) from the variation of potential energy $\delta\Pi$ with the variation of crack area δA due to the variation of the individual nodes along the crack front, use is made of the properties of isoparametric elements. Consider Fig. 11 representing a side of a parabolic isoparametric element lying on the crack front, with a local (x, y) coordinate system defined by nodes 1 and 3, and the generalised coordinate $\xi(-1 \leq \xi \leq 1)$. The crack front is defined by the relation for a side of a parabolic isoparametric element :

$$x = \frac{b}{2}(1+\xi) \quad , \qquad y = \left[1, \xi, \xi^2\right]\left[C\right]\left[y_1, y_2, y_3\right]^T \quad , \quad \left[C\right] = \frac{1}{2}\begin{bmatrix} 0 & 2 & 0 \\ -1 & 0 & 1 \\ 1 & -2 & 1 \end{bmatrix} \tag{16}$$

In a similar way δy and G are expressed as functions of nodal values, according to the concept of isoparametric elements:

$$\delta y = \left[1, \xi, \xi^2\right]\left[C\right]\left[\delta y_1, \delta y_2, \delta y_3\right]^T \tag{17}$$

$$G = \left[1, \xi, \xi^2\right]\left[C\right]\left[G_1, G_2, G_3\right]^T \tag{18}$$

(N. B. : G_1, G_2 and G_3 are not to be confounded with G_I, G_{II} and G_{III} for the various loading modes). Combining eq. (15), (16), (17) and (18), one obtains:

$$\left[\frac{\delta\Pi_1}{\delta y_1}, \frac{\delta\Pi_2}{\delta y_2}, \frac{\delta\Pi_3}{\delta y_3}\right]^T = \left[F\right]\left[G_1, G_2, G_3\right]^T \quad , \quad \left[F\right] = \frac{-b}{30}\begin{bmatrix} 4 & 2 & -1 \\ 2 & 16 & 2 \\ -1 & 2 & 4 \end{bmatrix} \tag{19}$$

For each element on the crack front similar equations result, which are assembled resulting into a system of N linear equations for the N nodal values G_i and as RHS the N variations of potential energy $(\delta\Pi_i)$ due to variation of position of node $i(\delta y_i)$.

APPENDIX 2

Although for the determination of energy release rates, the accuracy is less sensitive to the theoretical stress distribution around the crack tip, the application of singularity elements contributes to accuracy and as a consequence the mesh can be coarser[21-27]. In this paper

use is made of the property of isoparametric elements, having a singularity if the side nodes are not at their mathematically required position[25]. In particular for parabolic isoparametric elements with side nodes at one quarter of the crack tip node (Fig. 6) it can be shown that a $r^{-1/2}$ singularity exists for the strains at the crack tip node[26,28]. The remaining sides remain compatible with surrounding elements. Consider for this the side of an isoparametric element. The coordinate x is transformed into a generalised coordinate ξ according to:

$$x = \left[1, \xi, \xi^2\right] \left[C\right] \left[x_1, x_2, x_3\right]^T \quad , \quad \left[C\right] \text{ see eq. (16)} \tag{20}$$

For the standard configuration i.e. $x_1 = 0, x_2 = 1/2, x_3 = 1$ the mapping function (20) becomes:

$$x = \frac{1}{2}(1 + \xi) \rightarrow \xi = 2x - 1 \tag{21}$$

With the side node displaced i.e. $x_1 = 0, x_2 = 1/4, x_3 = 1$ one gets:

$$x = \frac{1}{4}(1 + \xi)^2 \rightarrow \xi = -1 + 2\sqrt{x} \tag{22}$$

For the displacements of the isoparametric element one can write:

$$u = \left[1, \xi, \xi^2\right] \left[C\right] \left[u_1, u_2, u_3\right]^T \tag{23}$$

The strain can be written as:

$$\varepsilon_x = \frac{\partial u}{\partial x} = \frac{\partial u}{\partial \xi} \frac{\partial \xi}{\partial x} \quad , \quad \varepsilon_x = u_1 g_1(x) + u_2 g_2(x) + u_3 g_3(x) \tag{24}$$

$$g_1(x) = 2 - 1.5\, x^{-1/2}, \quad g_2(x) = -4 + 2x^{-1/2}, \quad g_3(x) = 2 - 0.5\, x^{-1/2}$$

Equations (24) show the inverse square root strain singularity at x = 0. Moreover, a constant and a linear displacement field result in a zero, respectively constant strain and consequently the element can be used for thermal stress problems:

$$u_1 = u_2 = u_3 = 1 \rightarrow \varepsilon_x = g_1(x) + g_2(x) + g_3(x) \equiv 0 \tag{25}$$

$$u_1 = 0, \; u_2 = \frac{1}{4}, \; u_3 = 1 \rightarrow \varepsilon_x = \frac{1}{4} g_2(x) + g_3(x) \equiv 1 \tag{26}$$

TABLE I

SEQUENCE OF CALCULATIONS FOR 3D THERMO-ELASTIC CRACK PROBLEM IN NOZZLE. COSTS FOR IBM 370/165

RUN	MESH (Fig.)	PROGRAM	FUNCTION	Elements Nodes DOF	Band-width (DOF)	CPU (min)	EQ.CPU for I/0 (min)	EQ.CPU total (min)	COSTS at rate 1800 $/h
1	2, 3, 5	EURCRACK	MESH GENERATION	154, 124 1000, 1000 3000, 3000		0.15	0.18	.33	9.9
2	2	FLHE	THERMAL ANALYSIS OF NOZZLE (STEADY STATE)	160 1000 1000	95	2.07	0.45	2.52	75.6
3	2	BERSAFE-SUBSTRUCTURE	GENERATION OF SUBSTRUCTURE	160 1000 3000	285	16.20	1.45	17.65	529.50
4	3	FLHE	THERMAL ANALYSIS OF CRACK REFINEMENT	130 1000 1000	92	1.29	0.36	1.65	49.5
5	3	BERSAFE-SUBSTRUCTURE	ASSEMBLING OF SUBSTRUCTURE & BACK-SUBSTITUTION	130 1000 3000	276	10.05	0.8	10.85	325.5
6	5	BERSAFE-SUBSTRUCTURE	$[\delta K]$, $\{\delta f\}$ for 17 nodes on crack front	336 193 579	108	7.36	0.6	7.96	238.8
7		GCAL3	G(s)	17 nodes		0.5	0.5	1.00	30.
RUNS 1, 2, 3, 4, 5, 6, 7 FIRST			CRACK FRONT (THERMO-ELASTIC)			37.62	4.34	41.96	1258.8
RUNS 4, 5, 6, 7 SUBSEQUENT			CRACK FRONTS (THERMO-ELASTIC)			19.20	2.26	21.46	643.8
RUNS 1, 3, 5, 6, 7 FIRST			CRACK FRONT (ELASTIC)			34.26	3.53	37.79	1133.70
RUNS 5, 6, 7 SUBSEQUENT			CRACK FRONTS (ELASTIC)			17.91	1.9	19.81	594.30

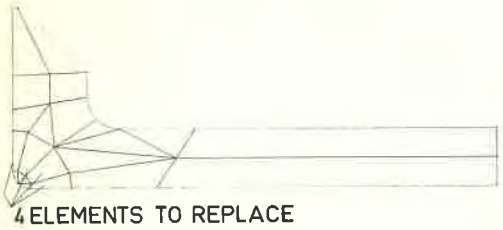

Fig. 1 2D Mesh of BWR nozzle

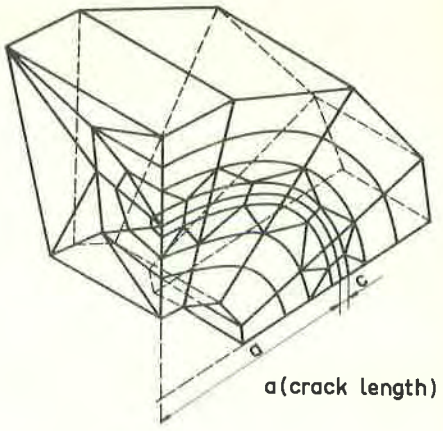

Fig. 3 3D Mesh refinement around crack

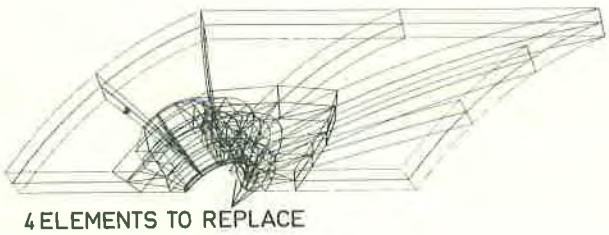

Fig. 2 3D Mesh of BWR nozzle

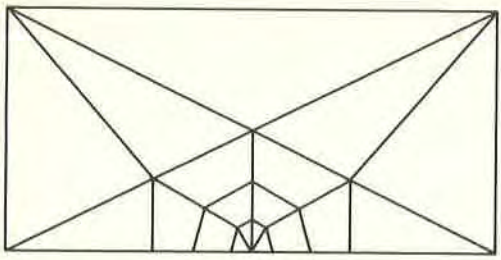

Fig. 4 2D Mesh refinement around crack

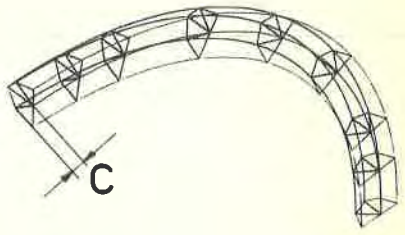

Fig. 5 3D Mesh of crack tip elements

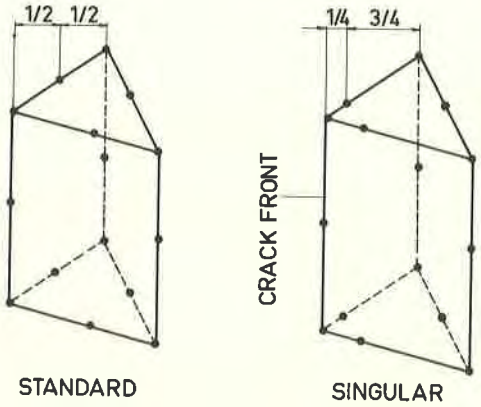

Fig. 6 Isoparametric wedge element (45 DOF)

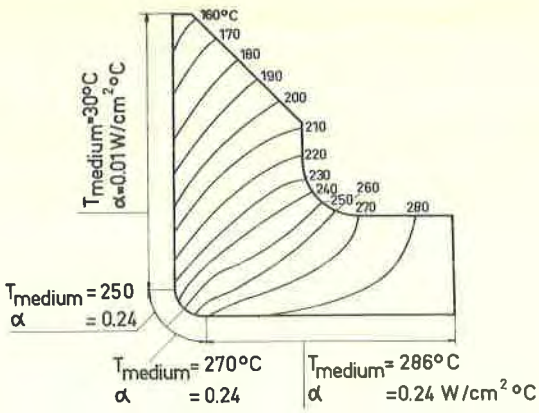

Fig. 7 Thermal boundary conditions and resulting temperature distributions

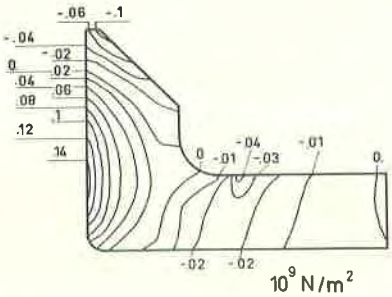

Fig. 8 Thermal stresses in uncracked nozzle

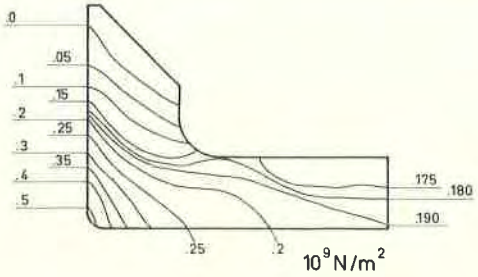

p = 90 bar

Fig. 9 Stresses due to internal pressure in uncracked nozzle

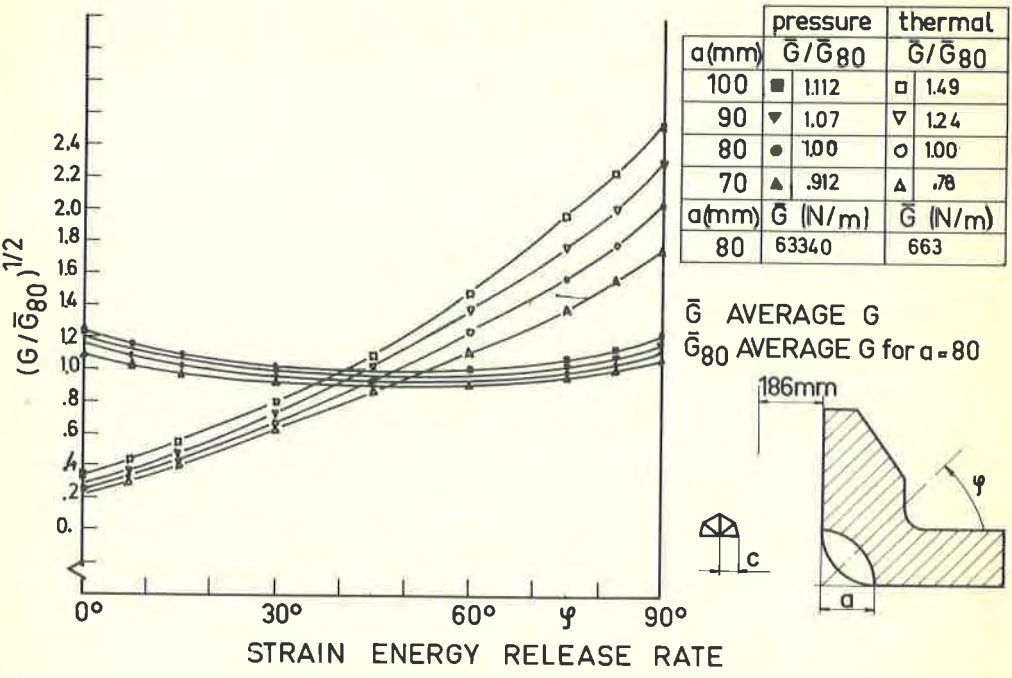

Fig. 10 G values along circular corner crack

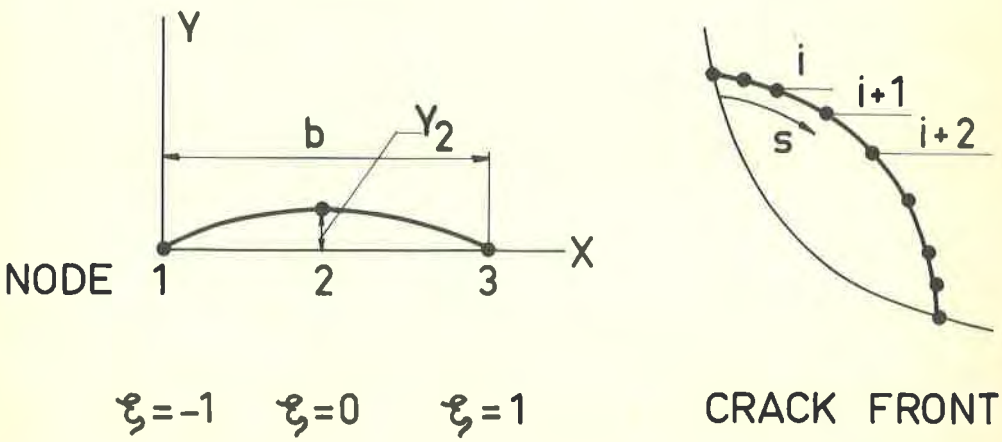

Fig. 11 Calculation of virtual crack area increase